AGU100 ADVANCING EARTH AND SPACE SCIENCE

JGR Atmospheres

RESEARCH ARTICLE
10.1029/2019JD031064

Key Points:
- Differences in shortwave radiative effects driven from different treatments of the transition zone have been investigated
- Three radiative parameterizations included in WRF-ARW, adapted for one-dimensional simulations, were used for this purpose
- Different treatments of the transition zone can lead to substantial differences in estimation of shortwave radiative effects at surface

Correspondence to:
B. Jahani,
babak.jahani@udg.edu

Citation:
Jahani, B., Calbó, J., & González, J.-A. (2019). Transition Zone Radiative Effects in Shortwave Radiation Parameterizations: Case of Weather Research and Forecasting Model (WRF). *Journal of Geophysical Research: Atmospheres*, *124*, 13,091–13,104. https://doi.org/10.1029/2019JD031064

Received 23 MAY 2019
Accepted 18 NOV 2019
Accepted article online 20 NOV 2019
Published online 4 DEC 2019
Corrected 17 FEB 2020

This article was corrected on 17 FEB 2020. See the end of the full text for details.

Transition Zone Radiative Effects in Shortwave Radiation Parameterizations: Case of Weather Research and Forecasting Model

Babak Jahani[1], Josep Calbó[1], and Josep-Abel González[1]

[1]Departament de Física, Universitat de Girona, Girona, Spain

Abstract A number of studies have stated that the shift from a cloud-free to cloudy atmosphere (and vice versa) contains an additional phase, named "Transition (or twilight) Zone". However, the information available about radiative effects of this phase is very limited. Consequently, in most meteorological and climate studies, the area corresponding to the transition zone is considered as an area containing aerosol or optically thin clouds. This study investigates the differences in shortwave radiative effects driven from different treatments of the transition zone. To this aim, three of the shortwave radiation parameterizations (NewGoddard, Rapid Radiative Transfer Model for Global circulation models, and Fu-Liou-Gu) included in the Advanced Research Weather Research and Forecasting Model (WRF-ARW) were isolated and adapted for one-dimensional vertical simulations. These parameterizations were then utilized to perform simulations under ideal "cloud" and "aerosol" modes, for different values of (i) cloud optical depths resulting from different sizes of ice crystals or liquid droplets and mixing ratios; and (ii) different aerosol optical depths combined with various aerosol types. The resulting shortwave broadband total, direct, and diffuse irradiances at the Earth surface were analyzed. The uncertainties originated from different assumptions of a situation regarding to the transition zone are quite substantial for all the parameterizations. For all the parameterizations, direct and total irradiances are the least and most sensitive irradiances to different treatments of the transition zone, respectively. Differences in the radiative effects of transition zone dominantly result from the difference between the radiative effects of clouds and aerosols (different types), not from cloud type or droplet/crystal size.

1. Introduction

Solar radiation is a key element of the Earth atmosphere system, and is involved in several natural processes. Furthermore, the amount of solar radiation reaching the Earth surface is mainly affected by aerosols and clouds, which are two particular cases of a single phenomenon, i.e. a suspension of particles in the air. However, the radiation-cloud-aerosol interactions are rather complex (Fan et al., 2016). Consequently, radiation, cloud and aerosol parameterizations may be considered as one of the most computationally demanding parts of the atmospheric, climate, and weather forecasting models (Carslaw et al., 2013). Thus, to this date a number of efforts have been made by researchers for studying and improving the radiation, cloud, and aerosol parameterizations in such models (Loeb et al., 2018; Ming & Held, 2018).

However, despite the existing differences in the origin and composition of clouds and aerosols, it is not always easy to clearly classify the type of suspension in the sky (González et al., 2017; Seinfeld et al., 2016). Indeed, the characteristics of the suspension sometimes lay on the border between those corresponding to a cloud and those corresponding to an atmospheric aerosol (Calbó et al., 2017). More precisely, the shift between cloudy to cloud-free atmosphere contains an additional phase named "Transition Zone" (also known as "Twilight Zone"), with characteristics that depend on both the nearby clouds and surrounding aerosols (Fuchs & Cermak, 2015; Koren et al., 2007). The situation gets even more complex when using data derived from measurements with relatively low temporal and/or spatial resolutions (Várnai & Marshak, 2011, 2015).

The transition zone may correspond to various processes including hydrated aerosols, cloud fragments sheared off from the adjacent clouds, decaying and incipient clouds, etc. (Koren et al., 2009). Moreover, studies show that the transition zone (as a property of a cloud field) may expand up to tens of kilometers away from the cloud field (Várnai & Marshak, 2011). According to Koren et al. (2007), almost 30-60% of the globe

categorized as clear sky (cloud-free) can potentially correspond to this phase. Based on the total cloud and aerosol records of the Moderate Resolution Imaging Radiometer satellite sensor between 2007 and 2011, Schwarz et al. (2017) concluded that almost 20% of all pixels could be categorized as transition zone. Calbó et al. (2017) quantified that the frequency of the transition zone is about 10%, on the basis of three ground-based observation systems at two mid-latitude sites. They also found that the transition zone produces typically an optical depth of less than 0.32, but it might be found, at those sites, for optical depth as high as 2.00. All these papers underline the fact that a significant proportion of sky at any time is covered by a particle suspension with characteristics of the transition zone, which seems to play, consequently, a significant role in the energy balance of the Earth. Despite the importance of the transition zone, however, the currently available information about its radiative effects and the mechanisms at which it influences the total climate system is limited. In most meteorological, climate, and weather forecasting studies and models, aerosols and clouds are commonly treated separately (as either dry aerosols or fully developed clouds), leaving no gap for the transition zone. This implies that, in the mentioned models, the condition of sky in each layer of a given grid cell is assumed to be either cloudy (fully or partially covered) or cloud-free (maybe containing aerosols), neglecting the transition zone.

The separate treatment of clouds and aerosols arises the question "how different the simulated radiative effects in a grid cell of a meteorological/weather forecasting model will be, if a situation corresponding to transition zone is assumed as cloud or aerosol?" Or in other words, "how important it is to study and deal with the radiative characteristics of the transition zone?" For this purpose, the present study aims to answer the mentioned questions by applying a sensitivity analysis to the shortwave radiation (swrad) parameterizations included in a particular meteorological model, namely the Weather Research and Forecasting Model (WRF), which is being widely used by meteorology organizations and research institutes all around the world.

2. Materials and Methods

2.1. Model Description

The Advanced Research WRF (WRF-ARW) is a state-of-the-art open source mesoscale atmospheric model, developed by National Center for Atmospheric Research (NCAR) for both research and numerical weather prediction purposes (Powers et al., 2017). This model, which is probably the most popular meteorological (it also has a climatic version) model worldwide, has the capability to be used for a wide range of applications, such as real-time numerical weather prediction, data assimilation, parameterized-physics research, regional climate simulations, air quality modeling, atmosphere-ocean coupling, and idealized simulations (Blossey et al., 2013; Doubrawa et al., 2018; Jimenez et al., 2016; Lin et al., 2015; Moeng et al., 2007; Montornès et al., 2016; Wang et al., 2009; Yamaguchi & Feingold, 2012; Zhong et al., 2016). In addition, it can be ran at different domains and offers various options for parameterization of convective processes, turbulent transports, evolution of surface temperature and soil moisture, and soil-air interactions (Ruiz-Arias et al., 2013; Skamarock et al., 2008). Similarly, WRF-ARW employs different frameworks for parameterization of swrad. However, the way these parameterizations deal with clouds and aerosols varies from one to another. They are also different in terms of other factors, such as required input data, spectral range, number of spectral bands, complexity of the calculations, etc. (Montornès et al., 2015).

The swrad parameterizations included in the latest version of WRF-ARW (Version 4.0) consist of: Dudhia (Dudhia, 1989), Fu-Liou-Gu (FLG, Gu et al., 2011), Goddard (Fels & Schwarzkopf, 1981), NewGoddard (Chou & Suarez, 1999), NCAR Common Atmosphere Model (CAM, Collins et al., 2006), Rapid Radiative transfer Model for Global circulation models (RRTMG), RRTMG-fast, RRTMG-K (Baek, 2017; Iacono et al., 2008), and Held-Suarez relaxation (Chen et al., 1997). However, among them, the parameterizations which (i) are more detailed and (ii) allow the users to consider different treatments of clouds and aerosol were chosen for this study. Thus, selected parameterizations comprise RRTMG, NewGoddard, and FLG. In these parameterizations, diffuse and direct irradiances are simulated separately, and then the total component is computed as the summation of diffuse and direct. However, these parameterizations involve different definitions of direct and diffuse irradiances: in the parameterizations NewGoddard and FLG, direct irradiance is a summation of scattering in forward direction and (eventually attenuated by absorption) direct beam, whereas for RRTMG the direct irradiance only refers to the direct beam. In the latter parameterization, scattering in all directions is considered as part of the diffuse component. More information about

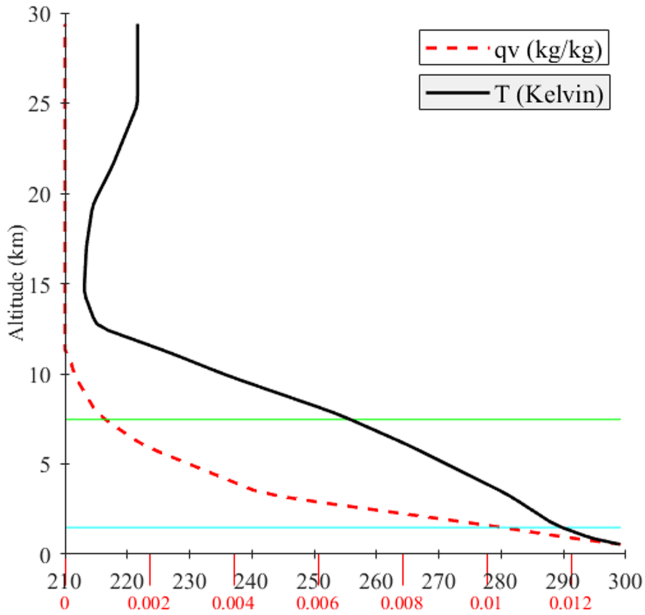

Figure 1. Vertical profiles of temperature T, (K, solid black line) and water vapor mixing ratio qv (kg/kg, red dashed line) used in the reference atmosphere (note: the blue and green line represent the average altitude of the liquid and ice clouds layers, respectively).

these parameterizations can be found in Skamarock et al. (2008) and Montornès et al. (2015), but a brief description follows:

1. RRTMG uses the two stream practical improved flux method (Zdunkowski et al., 1980) for solving the Radiative Transfer Equation (RTE). Furthermore, it considers the region between 0.20 μm and 12.20 μm wavelengths as the shortwave spectrum and splits into 14 spectral bands: 3 ultraviolet (UV), 2 PAR, and 9 near-infrared (IR). In this parameterization, ice and liquid cloud optical depths (ODs) are obtained as a function of the corresponding input mixing ratios and effective crystal/droplet sizes following the method provided by Fu (1996) and Hu and Stamnes (1993), respectively.
2. NewGoddard solves the RTE by using the two stream δ-Eddington approximation method (Joseph et al., 1976). In this parameterization, the swrad wavelength ranges between 0.18 μm and 10.00 μm, and it is divided into 11 spectral bands: 7 UV, one PAR, and 3 near-IR. NewGoddard computes the optical depth due to ice and liquid clouds based on Slingo and Schrecker (1982) method.
3. In terms of FLG, RTE is solved through the δ-four stream approximation method provided by Liou et al. (1988), and the region with wavelength between 0.20 μm and 4.00 μm is considered as shortwave spectrum. This parameterization splits this spectral region into 6 separate bands: one UV-PAR and 5 near-IR. FLG parameterizes ice and liquid cloud's ODs based on the method described in Slingo (1989).

These parametrizations have a different definition of the shortwave region. In addition, they also have a different distribution of spectral bands over the shortwave region. However, it should be noted that despite the shortwave region is extended up to 10.00 and 12.20 μm for parameterizations NewGoddard and RRTMG, none of the three parameterizations chosen deals with emission. This means that the irradiances calculated by these parameterizations are only affected by scattering and absorption. In order to be able to assess the performance of the radiation parameterizations independently of the other schemes of WRF-ARW and design simulations under ideal conditions, the source codes of these parameterizations were isolated from the main model structure and adapted for one dimensional vertical simulations ("sandbox" approach). By doing so, the inputs to the radiation parameterizations were given to the parameterizations under controlled conditions (regardless of the uncertainties associated with other parts of the model, such as microphysics). Consequently, the final results obtained from the radiation parameterizations will be affected only by the radiation parameterization itself. These isolated parameterizations were then utilized to perform several simulations under ideal "cloud" and "aerosol" modes.

2.2. Experiment Setup

To address the objectives of this study, conditions at midday for summer at mid-latitudes (46.8°) were selected, resulting in a solar zenith angle of ≈30°, and a standard mid-latitude summer time atmosphere was used (Anderson et al., 1986). A cloud- and aerosol-free (clean) atmosphere and a surface albedo of 0.14 was initially considered as a reference setup for all of the simulations. For all simulations, an equal number of 78 atmospheric layers were considered; the model top was set at 30 km. However, based on the results obtained for this reference model configuration, the same analysis was carried out later for different values of solar zenith angles and surface albedos (a summary of results obtained for these additional configurations is provided in the Discussion Section). Figure 1 shows the vertical profiles of air temperature (T) and water vapor mixing ratio (qv) in the reference atmosphere.

The isolated parameterizations were used to simulate the shortwave broadband direct (horizontally projected), diffuse, and total irradiances at Earth surface by adding to the reference setup (i) ice and liquid clouds with different ODs resulting from different crystal and droplet sizes and water contents; and (ii) aerosols with different ODs combined with various aerosol types. In all these simulations the cloud/aerosol OD was considered to vary between 0.01 and 2.00. This range of OD covers low and high values of OD which can

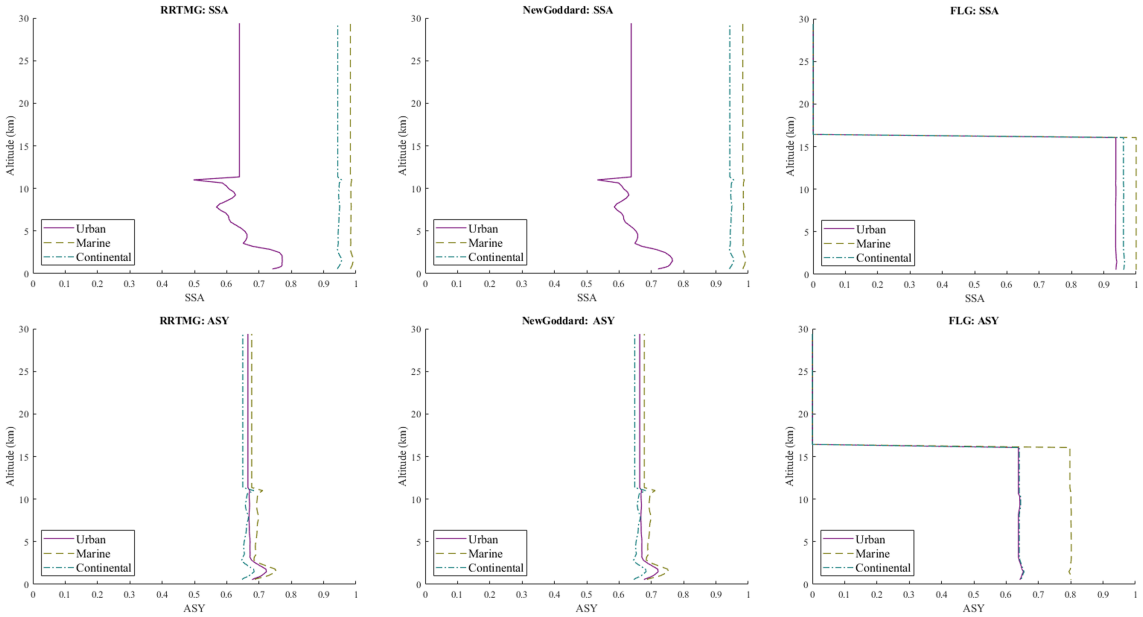

Figure 2. Vertical profiles of SSA (top panel) and ASY (bottom panel) for the pre-described urban, continental and marine aerosol models included in the parameterizations RRTMG, NewGoddard and FLG.

potentially represent a situation regarding to the transition zone. Also, it contains the typical range of OD for the transition zone that Calbó et al. (2017) found for two sites located in unpolluted regions.

The cloud altitude for the liquid and ice clouds was considered to be ~1.5 km and ~7.5 km, respectively. The effective radius of cloud ice crystals was considered to vary between 10 and 120 μm. Similarly, the effective radius of cloud droplets was considered to vary between 2.5 and 15 μm. These cases comprise 11 combinations (four ice and four liquid clouds and three aerosol types) for each considered OD. As each of the parameterizations selected uses different methods and coefficients for calculation of cloud OD, the cloud OD for all crystal and droplet sizes were obtained through trial and error: fixing droplet/crystal size and increasing/decreasing water/ice mixing ratio until the desired OD (at the band that contains the 0.550 μm wavelength) with a maximum error of ±1% is obtained.

The aerosol types used in this study consist of three predescribed aerosol models which are common among all parameterizations selected: (1) urban; (2) continental; and (3) marine. Among them, the marine and urban aerosols are the most reflective and absorbing aerosols, respectively. In these parameterizations, the aerosol OD at 0.550 μm and the desired aerosol type are given to the parameterization as an input. Then, based on the aerosol type selected, the parameterizations use the predescribed aerosol models included in them to distribute the aerosols' optical properties (OD, single scattering albedo and asymmetry factor) for all of the spectral bands along the column of the atmosphere. For all parameterizations and aerosol types, aerosols are mostly concentrated in the lower layers (< 3 km) of the atmosphere, decaying exponentially with height. It is worth mentioning that the other optical characteristics of these aerosol types and their distribution along the column of the atmosphere are defined differently by each parameterization: there are minor differences between RRTMG and NewGoddard, while those of FLG are remarkably different compared with the other parameterizations. The information regarding to the values and distributions of an aerosol single scattering albedo (SSA) and asymmetry factor (ASY) of the three parameterizations at the spectral bands containing the 0.550 μm wavelength have been extracted from the source codes of the parameterizations and provided in Figure 2.

2.3. Quantification of Radiative Effects and Sensitivity

In order to be able to have a clear insight about the differences among irradiances, which may only arise from different treatments of the transition zone (i.e., description as cloud or as aerosol), and eliminate the effect of other factors which may affect the broadband direct, diffuse, and total irradiances at the Earth's

surface (ozone, trace gases, water vapor, etc.); the radiative effects for the mentioned irradiances under each model run were calculated through equation (1):

$$RE_{\alpha,irr,par}\,(OD) = E_{\alpha,irr,par}\,(OD) - E_{irr,par}(0) \quad (1)$$

where $RE_{\alpha,irr,par}$ (OD) (W m^{-2}) is the radiative effect for irradiance *irr* (total, direct, and diffuse) for the αth run (α = 1-11) for the parameterization *par* at a given OD. $E_{\alpha,irr,par}$ (OD) (W m^{-2}) is the computed irradiance *irr* for the αth run of the parameterization *par* at a given OD; $E_{irr,par}(0)$ stands for the irradiance *irr* computed by the parameterization *par* under the reference configuration (cloud- and aerosol-free atmosphere, OD = 0). These radiative effects were then utilized in the further analysis.

Nevertheless, in order to be able to provide comparisons among the radiative effects and to quantify the ranges at which they may vary for different treatments of the transition zone (a comparison between ice clouds and aerosols, I-a; and another between liquid clouds and aerosols, L-a), two additional indices; the Radiative Effect Range (ΔRE, W m^{-2}) and the Mid-range Radiative Effect ($\overline{RE}$), were proposed:

$$\Delta RE_{irr,par}\,(OD) = Max\left(RE_{\alpha,irr,par}\,(OD)\right) - min\left(RE_{\alpha,irr,par}\,(OD)\right) \quad (2)$$

$$\overline{RE}_{irr,par}\,(OD) = \left[Max\left(RE_{\alpha,irr,par}\,(OD)\right) + min\left(RE_{\alpha,irr,par}\,(OD)\right)\right]/2 \quad (3)$$

where $\Delta RE_{irr,par}$ (OD) and $\overline{RE}_{irr,par}$ (OD) (W m^{-2}) take into account the dispersion of all radiative effects for the cases I-a (three aerosol types and four ice clouds, α = 3 + 4) and L-a (three aerosol types and four liquid clouds, α = 3 + 4), produced by the parameterization *par*, for the irradiance *irr* at a given OD. It should be noted that hereafter the range will also be called "sensitivity," as this measure of the dispersion of results for a given OD indicates the error that may be involved with using one particular treatment of the transition zone. Here, $\overline{RE}$ has been calculated as an average of the minimum and maximum REs for (i) simplicity and (ii) in order to avoid giving extra weight to the values produced by cloud or by aerosol treatment. This way, $\overline{RE}$ is just in the midpoint between the maximum and minimum RE values at a given OD, so in the middle of the range of values where the actual RE should lay. Therefore, this midrange value is appropriate to be used for normalizing the range (see below).

However, due to the differences in the magnitude of the radiative effects (mainly depending on OD), equations (2)–(3) fail to show the importance of the sensitivity in relation to the corresponding parameterizations. For this reason, a relative index, the Relative Radiative Effect Sensitivity (RΔRE, %, equation [4]) was introduced as well:

$$R\Delta RE_{irr,par}\,(OD) = 100\times\left[\Delta RE_{irr,par}\,(OD)/\left|\overline{RE}_{irr,par}\,(OD)\right|\right] \quad (4)$$

Moreover, in order to represent the relative sensitivity in a bulk single number for the whole range of ODs, the Mean Relative Radiative Effect Sensitivity ($\overline{R\Delta RE}$, equation 5) was also defined as follows:

$$\overline{R\Delta RE}_{irr,par} = \frac{1}{OD_{max} - OD_{min}} \times \int_{OD_{min}}^{OD_{max}} R\Delta RE_{irr,par}(OD)\,dOD \quad (5)$$

Thus, variables $R\Delta RE_{irr,par}$ (OD) and $\overline{R\Delta RE}_{irr,par}$ (%) provide quantitate information about the ΔRE regarding to each parameterization in relation to the corresponding radiative effect simulated by the parameterization for a given and for the whole range of OD, respectively. In some way, these values are useful as a first estimation of the uncertainty that is involved when dealing with radiative effects of a transition zone situation.

3. Results

3.1. Radiative Effects (RE)

An overall picture about the variations of direct (RE_{dir}), diffuse (RE_{dif}), and total (RE_t) radiative effects of the atmosphere resulting from different treatments of transition zone, based on the model simulations, is provided in Figure 3. In this figure, the upper panel shows comparison between the REs of ice clouds and

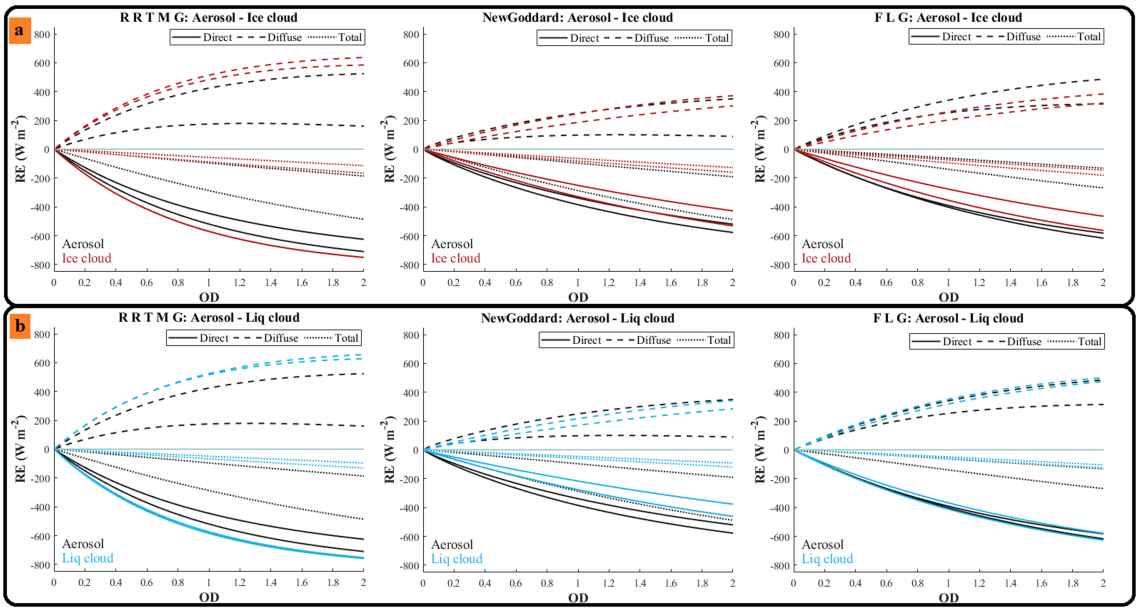

Figure 3. Minimum and Maximum values of RE_{dir}, RE_{dif} and RE_t of the atmosphere resulted from different treatments of transition zone versus OD (0.01-2.00), based on NewGoddard, RRTMG and FLG simulations for cases I-a (panel "a") and L-a (panel "b").

aerosols (I-a), and the lower panel shows the comparison between the REs of liquid clouds and aerosols (L-a). Furthermore, the lines of the same type and color correspond to the maximum and minimum possible values of RE_{dir}, RE_{dif}, and RE_t due to aerosols, ice, and liquid clouds for OD between 0.01 and 2.00, based on each parameterization. Therefore, for each case (I-a and L-a) the distance between the lowest and highest lines of the same type is the range of dispersion (ΔRE) of the simulated values of RE_{dir}, RE_{dif}, and RE_t, based on the different treatments of the transition zone. According to this figure, for all parameterizations and for both comparison cases, the increment in the aerosol/cloud OD leads to reduction and enhancement of direct and diffuse irradiances, respectively, resulting in a decrease in total irradiance. In addition, the declining rate of RE_{dir} versus OD seems to be higher in RRTMG compared to the two other parameterizations. The lines for RRTMG given in Figure 3 are more concave, meaning that the decrease is particularly steeper for lower OD (<1.00). For the two other parameterizations, RE_{dir} appears to have almost similar rate of variation versus OD. This may be due to the difference in the definition of direct irradiance among the parameterizations; as above mentioned, direct irradiance is defined as the summation of direct beam and forward scattering in NewGoddard and FLG, while in RRTMG, direct irradiance only refers to the direct beam. Furthermore, from Figure 3 it can be seen that the effect of droplet/crystal size on the simulated RE_{dir} and RE_{dif} seem to be different depending on the parameterization utilized. Its effect, however, is generally smaller on RE_t for all the parameterizations.

According to this figure, there is a substantial difference among the REs (all components) simulated by the parameterization FLG for the liquid and ice clouds. This difference can be more visibly seen in RE_{dif} compared to other components of solar radiation. Furthermore, based on this parameterization liquid clouds have higher RE_{dir} and RE_{dif} (absolute values) compared to the ice clouds. Also, the effect of particle (crystal/droplet) size (the distance between the highest and lowest values) is larger for ice clouds, compared to liquid clouds This may be due to the larger range of ice crystal sizes considered in our simulations compared to liquid droplets, because larger particles imply enhanced forward scattering (Bohren & Huffman, 1998; Petty, 1958), and thus more (less) radiation in the direct (diffuse) component. In contrast, the parameterization FLG projects very similar RE_{dir} for the three different aerosol types, so only at the higher ODs the differences are visible in Figure 3. Moreover, the magnitude of RE_{dir} simulated by FLG for aerosols is also similar to that of the liquid clouds with large droplet size, in particular at the lower ODs. However, there are more differences among the RE_{dif} simulated by this parameterization for the three aerosol types. According to the simulations of this parameterization, the RE_{dif} of aerosols may be similar to that of ice

cloud or liquid cloud, depending on the aerosol type. However, the magnitude of RE_t corresponding to aerosols (depending on the aerosol type) can either be similar to or greater (in absolute sense) than that of clouds.

In case of the parameterization NewGoddard, although it produces some differences between ice and liquid clouds, it projects the same RE_{dir} and RE_{dif} for liquid clouds with small droplet sizes and ice clouds with large crystal sizes at the same OD (Figure 3). This parameterization produces lower RE_{dir} and RE_{dif} (absolute values) for the liquid clouds compared to the ice clouds, unlike FLG. Contrarily, and similar to FLG, this parameterization produces distinct RE_t for ice and liquid clouds. The effect of particle (crystal/droplet) size is, however, smaller compared to FLG. Also, for OD < 0.50 the RE_{dif} simulated by this parameterization for the aerosols is very similar to that of the clouds. However, for OD > 0.50, RE_{dif} simulated by NewGoddard for aerosols (depending on the type) may either be very similar or very different from that of both cloud types. Although the RE_{dir} simulated by this parameterization for the aerosols is generally greater than that of the clouds, however, it projects similar RE_{dir} for clouds with small crystal sizes and a particular type of aerosols (continental). In terms of total radiation, Figure 3 shows a vast difference among the REs of clouds and aerosols simulated by the parameterization NewGoddard, even at very low OD (0.10): those corresponding to the aerosols are greater (in absolute sense) than those of the clouds.

Unlike the two other parameterizations discussed, RRTMG produces almost the same RE_{dir} for different types of ice and liquid clouds resulting from different droplet/crystal sizes (Figure 3). This implies that the RE_{dir} simulated by the parameterization RRTMG is not very sensitive to different treatments of clouds, at least at this limited range of low OD. However, it is worth mentioning that RRTMG projects a higher extinction rate of RE_{dir} for clouds compared to the two other parameterizations studied: for example, at OD = 1.00, RE_{dir} for both liquid and ice clouds is approximately 575 W m^{-2}. The simulated values of RE_{dif} show that the parameterization RRTMG considers some differences between the two cloud types, which do not appear to be substantial, though. In addition, it can also be seen that cloud particle size has more influence on the RE_{dif} simulated by RRTMG for ice clouds, compared with that of liquid clouds. In case of total irradiance, although the parameterization RRTMG produces differences between the RE_t of the two cloud types, it simulates similar RE_t for the liquid clouds with small droplet sizes and ice clouds with large crystal sizes. Moreover, similar to diffuse irradiance, cloud particle size seems to have more influence on the RE_t regarding to ice clouds, compared to that of liquid clouds. In contrast, from the data represented in Figure 3 it can be seen that the parameterization RRTMG considers a vast difference between the RE (all components) of different aerosol types compared to the cloud types. This fact shows that the parameterization RRTMG is more sensitive to aerosol characteristics compared to those of clouds. Also, it produces less RE_{dif} and RE_{dir} (in absolute sense) for aerosols compared to clouds, which combined produce, however, a greater effect (in absolute sense) on the total irradiance. It is worth mentioning that this difference between the RE of clouds and aerosols increases with OD.

3.2. Sensitivities (ΔRE)

The values of ΔRE_{dir}, ΔRE_{dif}, and ΔRE_t for each of the parameterizations versus OD are provided in Figure 4. Based on the $\overline{R\Delta RE}$ values also shown in Figure 4, it can be affirmed that in all the parameterizations studied, RE_{dir}, and RE_t are the least and most sensitive variables to different treatments of transition zone. However, in an absolute sense, for the parameterizations RRTMG and FLG, RE_{dif} is the most sensitive component. It is worth mentioning that despite the direct component being the least sensitive to the transition zone treatment, ΔRE_{dir} still seems to be notable ($\overline{R\Delta RE}_{dir,I-a}$ = 44, 25 and 38%, $\overline{R\Delta RE}_{dir,L-a}$ = 57, 27, and 11% for parameterizations NewGoddard, RRTMG, and FLG, respectively).

As shown in Figure 4, the values of $\Delta RE_{dir,I\text{-}a}$ and $\Delta RE_{dir,L\text{-}a}$ resulted from the simulations of the three parameterizations nonlinearly vary with OD. In case of the parameterizations NewGoddard and FLG, $\Delta RE_{dir,I\text{-}a}$ and $\Delta RE_{dir,L\text{-}a}$ continuously increases with OD for the whole range of OD studied. This increase, however, is steeper for lower OD (<1.00). In contrast, for RRTMG, Figure 4 shows an increase and a slight decline in $\Delta RE_{dir,I\text{-}a}$ and $\Delta RE_{dir,L\text{-}a}$ for ODs ranged 0.01–1.00 and 1.00–2.00, respectively. The rapid extinction of the direct component in RRTMG (specially for lower range of OD) may be a possible reason for this particular behavior observed in $\Delta RE_{dir,I\text{-}a}$. From Figure 4, it can also be seen that there are slight differences among values of $\Delta RE_{dir,I\text{-}a}$ resulted from the simulations of all parameterizations. For $\Delta RE_{dir,L\text{-}a}$, however, there are more substantial differences among the parameterizations. This means that although all the

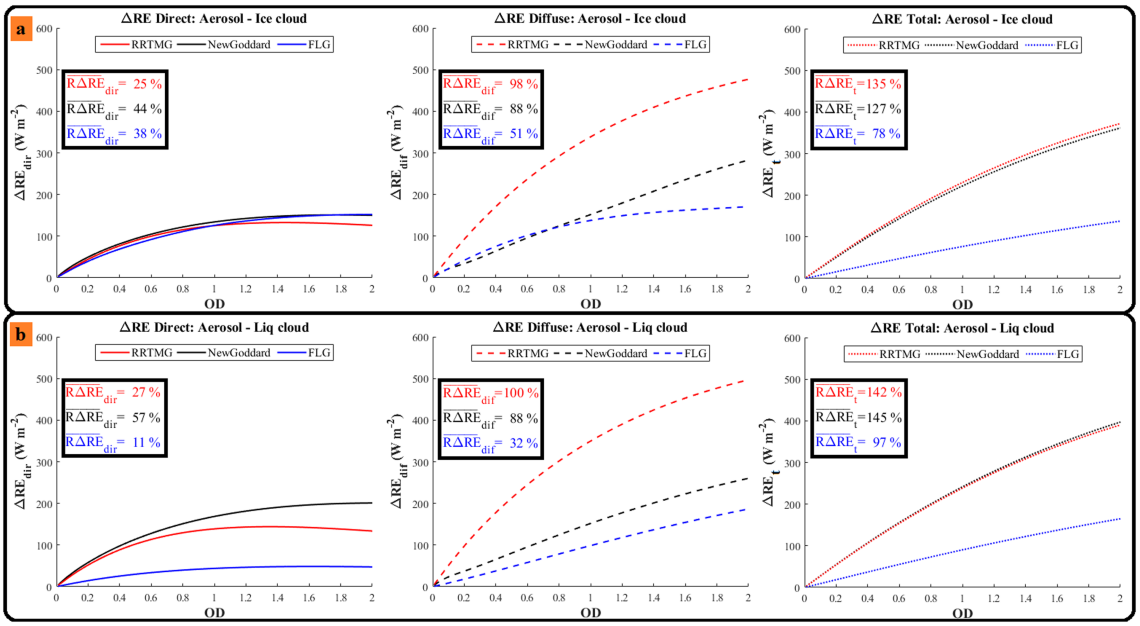

Figure 4. values of ΔRE_{dir}, ΔRE_{dif}, and ΔRE_t versus OD (0.01–2.00), based on RRTMG, NewGoddard and FLG simulations for cases I-a (panel "a") and L-a (panel "b"). Note: the values of $\overline{R\Delta RE}_{dir}$, $\overline{R\Delta RE}_{dif}$ and $\overline{R\Delta RE}_t$ with respect to each parameterization are also presented in this figure.

parameterizations are almost equally sensitive to different treatment of the transition zone under the case I-a, there are quite vast differences among their sensitivities under the case L-a. This difference can be more visibly seen in the parameterization FLG. In case of this parameterization, $\Delta RE_{dir,I\text{-}a}$ varies between 2 and 152 W m^{-2}, whereas $\Delta RE_{dir,L\text{-}a}$ varies between 1 and 48 W m^{-2} for the range of OD studied. In contrast, for NewGoddard, the values of $\Delta RE_{dir,L\text{-}a}$ (4-201 W m^{-2}) are higher than those of $\Delta RE_{dir,I\text{-}a}$ (3-150 W m^{-2}). Unlike the two other parameterizations, RRTMG is almost equally sensitive under both cases ($\Delta RE_{dir,L\text{-}a}$ and $\Delta RE_{dir,I\text{-}a}$ show similar values).

According to Figure 4, although the ΔRE_{dif} regarding to all parameterizations increases with OD for both cases, the values corresponding to the case I-a are slightly greater than those of L-a, implying that there are very small differences among the models sensitivities in simulation of diffuse irradiance for both cases. This figure also shows that $\Delta RE_{dif,I\text{-}a}$ and $\Delta RE_{dif,L\text{-}a}$ values resulting from RRTMG simulations increase nonlinearly with OD and their magnitudes at any OD are clearly higher than those of the two other parameterizations. In addition, these values are also higher than the corresponding values of ΔRE_{dir} resulting from RRTMG simulations, which imply higher sensitivity in diffuse compared to the direct. More precisely, different treatments of transition zone under the case I-a seem to lead to a wider range of results for the diffuse component of solar radiation compared to direct for the parameterization RRTMG. In case of the parameterization FLG, despite $\Delta RE_{dif,I\text{-}a}$ and $\Delta RE_{dif,L\text{-}a}$ having almost the same values for the range of OD studied, they have different variation patterns; $\Delta RE_{dif,I\text{-}a}$ varies nonlinearly and the other linearly. The magnitude of the $\Delta RE_{dif,I\text{-}a}$ resulted from the simulations of the parameterization FLG more or less varies in the same range as $\Delta RE_{dir,I\text{-}a}$ does (specially for OD < 1.00). But, comparing them with the corresponding midpoint radiative effects, the relative sensitivity of this parameterization to simulation of the diffuse component at the transition zone is higher than the direct ($\overline{R\Delta RE}_{dif,I-a} = 51\%$, $\overline{R\Delta RE}_{dif,I-a} = 38\%$). This figure also shows a substantial difference between the $\Delta RE_{dir,L\text{-}a}$ and $\Delta RE_{dif,L\text{-}a}$ resulting from FLG simulations. For the parameterization NewGoddard, in contrast, the ΔREs for both cases vary linearly and they have very similar values in the range of OD studied. In both cases (I-a and L-a), the ΔRE_{dif} values resulting from NewGoddard simulations are greater than those of ΔRE_{dir}, but this difference can be more clearly be seen in the case I-a.

In case of total irradiance, as Figure 4 shows both $\Delta RE_{t,I\text{-}a}$ and $\Delta RE_{t,L\text{-}a}$ values with respect to all parameterizations vary nonlinearly for the range of OD studied. This nonlinear behavior can be more clearly seen for

Table 1
Direct, diffuse, and total irradiances (W m^{-2}) simulated by the parameterizations NewGoddard (N.G.), RRTMG and FLG for reference aerosol- and cloud-free atmosphere configurations: (i) solar zenith angle~30° and surface albedo = 0.14 (ref), (ii) solar zenith angle~30° and surface albedo = 0.04 (ALB_4), (iii) solar zenith angle~30° and surface albedo = 0.40 (ALB_40), and (iv) solar zenith angle~60° and surface albedo = 0.14 (SZA_60)

	Direct			Diffuse			Total		
Configuration	N.G.	RRTMG	FLG	N.G.	RRTMG	FLG	N.G.	RRTMG	FLG
ref	848	835	872	55	55	61	903	890	933
ALB_4	848	835	872	47	50	54	897	884	926
ALB_40	848	835	872	71	70	81	919	905	953
SZA_60	414	405	427	45	45	49	459	450	476

ODs greater than 1.00. Based on Figure 4, at any given OD, despite the differences observed in the diffuse and direct irradiances simulated by the parameterizations RRTMG and NewGoddard, the summation of these two components produce mostly the same values of $\Delta RE_{t,I\text{-}a}$ and $\Delta RE_{t,L\text{-}a}$ for both parameterizations. This implies that the parameterizations NewGoddard and RRTMG have a similar sensitivity to simulation of the total irradiance in the transition. The data regarding to $\overline{R\Delta RE}$ given in Figure 4 also proves this fact. From Figure 4, it can also be seen that there is a substantial difference between the values of $\Delta RE_{t,I\text{-}a}$ and $\Delta RE_{t,L\text{-}a}$ that resulted from the simulations of FLG and those of the two other parameterizations. More precisely, at any given OD, the ΔRE_t of NewGoddard and RRTMG are more than twice as much as that of FLG. This implies that the total irradiance simulated by FLG is much less sensitive to different treatments of the transition zone under both cases compared with the two other parameterizations.

4. Discussion

The simulations of all the parameterizations studied show that for all the treatments (different clouds and aerosol types) RE_{dir} and RE_t decrease (i.e. reach negative values that are greater in absolute terms) and RE_{dif} increases with OD, which is to be expected due to enhanced absorption and scattering at higher ODs. However, REs (at any given OD) for each treatment and the rate at which they vary versus OD may be different depending on the parameterization utilized. Similarly, the ΔRE (all components) involved with the simulation of the radiative effect of a situation corresponding to the transition zone is different depending on the parameterization utilized. The differences in the treatment of forward scattering, number of spectral bands, and range of shortwave spectral region considered by the parameterizations, the methods used for solving the RTE and for cloud/aerosol parameterization as well as the code accuracy (Huang & Wang, 2019) may be reasons for these differences detected among the parameterizations. Indeed, Table 1 shows the irradiances simulated by the three parameterizations under the reference (aerosol- and cloud-free) configuration, and the remarkable difference among parameterizations is obvious, so confirming that some of the former reasons play an important role.

The parameterization RRTMG gives mostly similar REs for ice and liquid clouds with different particle sizes (especially in direct irradiance). However, it gives very different REs for different aerosol types. In addition, the parameterization RRTMG simulates completely different REs for clouds and aerosols. More precisely, despite RE_{dir} with respect to aerosols is slightly lower than that of clouds (in terms of the absolute values), the resulting RE_t regarding to aerosols is much less (i.e., greater in absolute terms) than that of clouds. This may mainly be due to the way diffuse component is described by this parameterization for clouds and aerosols. In other words, the parameterization RRTMG seems to project quite different rates of scattering for aerosols and clouds at any OD. According to the simulations of this parameterization, the difference in the RE take the lowest and highest values for direct ($\overline{R\Delta RE}_{dir,I-a}$ = 25% and $\overline{R\Delta RE}_{dir,L-a}$ = 27%) and total ($\overline{R\Delta RE}_{t,I-a}$ = 135% and $\overline{R\Delta RE}_{t,L-a}$ = 142%) irradiances, respectively. This notable uncertainty observed in the total irradiance, mainly originates from the uncertainty associated with simulation of diffuse irradiance at the transition zone ($\overline{R\Delta RE}_{dif,I-a}$ = 98% and $\overline{R\Delta RE}_{dif,L-a}$ = 100%). If we assume the whole atmosphere as one atmospheric layer, according to the equation 3 given in Menang (2018) the shortwave heating rate (H, K day^{-1}) for the whole column of the reference atmosphere (ΔP = 956 hPa) based on RRTMG simulations would be equal to 2.10 K day^{-1}. Accordingly, the different treatment of the transition zone at OD = 1.00

will result in a H dispersion range (ΔH) of about 2.50 and 2.43 K day^{-1} for the cases I-a and L-a, respectively. Furthermore, these differences in the RE of transition zone result from the difference between the RE of clouds and aerosols, not from different cloud droplet/crystal size and water/ice content. This means that according to RRTMG simulations, by assuming the fact that the RE of transition zone is the same as that of a layer of (i) cloud, (ii) aerosol, or a (iii) mixture of both, the uncertainty involved with not considering the actual RE of the transition zone can be rather high, especially for diffuse and total irradiances. It is, however, worth mentioning that it is generally believed that total irradiance is less sensitive to aerosol optical properties compared to direct and diffuse irradiances (Ruiz-Arias et al., 2013) and that some numerical weather prediction models do not consider aerosols in the simulation of RE (Jimenez et al., 2016).

Unlike RRTMG, there are distinct differences among the direct and total REs simulated by the parameterization NewGoddard for ice and liquid clouds with different particle sizes. For diffuse component, however, this parameterization projects small differences among the REs of ice and liquid clouds. The projected differences among the REs of clouds of different type with different particle sizes were expected due to the fact that this parameterization was in principle developed for studying the role of clouds and their interactions with radiation in climate and hydrological systems and later the impact of aerosols was added to it (Tao et al., 2009). Based on NewGoddard simulations, a substantial difference in the REs resulted from different treatments of a situation corresponding to transition zone can be seen in almost all of the irradiances evaluated. This difference, however, can be more notably seen in total irradiance ($\overline{R\Delta RE}_{dir,L-a}$ = 57%, $\overline{R\Delta RE}_{dif,L-a}$ = 88% and $\overline{R\Delta RE}_{t,L-a}$ = 145%). According to the simulations of this parameterization, the H regarding to the reference atmosphere is 1.87 K day^{-1} and the corresponding values of ΔH for I-a and L-a at OD = 1.00 are 2.48 and 2.41 K day^{-1}. The differences observed in the RE_{dif} and RE_t of transition zone are generally due to the difference in the REs regarding aerosols and clouds (similar to RRTMG), but the difference observed in RE_{dir} seems to be mainly owing to difference in the REs of the clouds of different type with various particle sizes. It is worth mentioning that the parameterization NewGoddard may produce mostly similar RE_{dif} for clouds and aerosols of marine and urban origins. However, there is a distinct difference among the RE_{dir} and RE_t simulated for clouds and aerosols.

The parameterization FLG is less sensitive to different treatments of the transition zone compared with the two other parameterizations. But still it has a relatively high sensitivity to different treatments of the transition zone ($\overline{R\Delta RE}_{t,L-a}$= 97% and $\overline{R\Delta RE}_{t,I-a}$=78%). According to FLG simulation, H for the reference atmosphere is equal to 1.77 K day^{-1}, and the corresponding values of ΔH for I-a and L-a at OD = 1.00 are 0.76 and 0.67 K day^{-1}. The parameterization FLG also reveals a distinct difference among the ice and liquid clouds (for all of the irradiances). It also projects different REs for clouds of the same type but with different particle sizes. The difference among the REs regarding to the two cloud types is larger in diffuse and total compared to the direct. The RE_{dir} regarding to aerosols (all types) is very similar to those of liquid clouds. Also, the RE_{dif} regarding to the liquid clouds simulated by this parameterization has a value similar to that of the marine aerosols. A similar pattern is also visible in RE_t; for OD between 0.01 and 2.00, the RE_t simulated by FLG for the ice and liquid clouds is very similar to that of marine aerosols.

All results shown and discussed so far correspond to a particular atmospheric profile, Sun position and ground albedo. In order not to be restricted to these specifications, the same analysis was carried out for a solar zenith angle of about 60°, and for a surface albedo of 0.04 and 0.40. Figure 5 provides a comparison among the values of $\overline{R\Delta RE}_{dir}$, $\overline{R\Delta RE}_{dif}$, and $\overline{R\Delta RE}_t$ that resulted from the simulations of the parameterizations NewGoddard, RRTMG, and FLG under the mentioned conditions. In this figure, the former configuration (solar zenith angle≈30° and surface albedo = 0.14) is considered as the reference setup. Information regarding to direct, diffuse, and total irradiances simulated by the parameterizations for the aerosol- and cloud-free atmosphere setups for these additional cases (solar zenith angle of about 60°, and for surface albedos of 0.04 and 0.40) is given in Table 1. Again, it should be noted the important differences among the three radiation schemes, as previously noted for the reference setup.

Figure 5 suggests that despite the uncertainties involved with different treatments of the transition zone change depending on the solar zenith angle and surface albedo, they still remain substantial. It also shows that in almost all cases (all except the direct and diffuse irradiances simulated by FLG), all the parameterizations studied the have slightly higher sensitivities under the case L-a than I-a. From the information

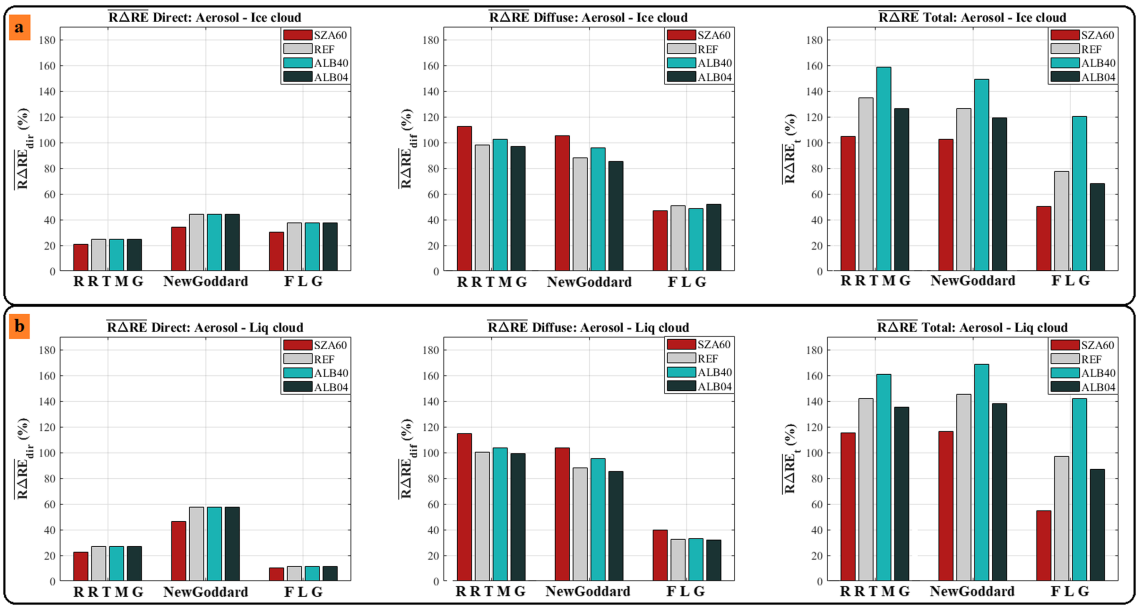

Figure 5. The values of $\overline{R\Delta RE}_{dir}$ (direct, left), $\overline{R\Delta RE}_{dif}$ (diffuse, middle) and $\overline{R\Delta RE}_{t}$ (total, right) resulted from RRTMG, NewGoddard, and FLG simulations for the cases I-a (panel "a") and L-a (panel "b") for (i) the reference setup (REF, gray), (ii) solar zenith angle~60° and surface albedo = 0.14 (SZA_60, red) and (iii) solar zenith angle~30° and surface albedo = 0.04 (ALB_4, dark green), and (iv) solar zenith angle~30° and surface albedo = 0.40 (ALB_40, light green).

provided in Figure 5, it can be realized for all parameterizations, under all model configurations (different solar zenith angles and surface albedos) total irradiance is the most sensitive irradiance to different treatments of the transition zone. Given the facts that (i) most weather prediction models internally need the total irradiance in the model's energy budget (Jimenez et al., 2016) and (ii) a large proportion of the cloudless atmosphere may potentially represent the transition zone (Koren et al., 2007; Schwarz et al., 2017), we can speculate that the confusion involved with the cloud-aerosol transition zone may introduce large biases in other parts of the models.

Based on Figure 5, for all configurations evaluated, the parameterizations NewGoddard and RRTMG, respectively, showed the highest and lowest sensitivity in the direct component. In terms of diffuse irradiance, (under all configurations) parameterizations RRTMG and FLG, respectively, had the highest and lowest sensitivity to different treatments of the transition zone. The difference between the $\overline{R\Delta RE}_{dif}$ with respect to NewGoddard and RRTMG under different configurations, however, is very small. These two parameterizations also present similar (and high) sensitivity to different treatments of the transition zone in total irradiance.

Figure 5 also shows that the change in the surface albedo has no effect on the sensitivity in direct irradiance, which is to be expected because physically the surface albedo has no influence on the direct beam, unlike what happens on diffuse (and therefore, on total) irradiances. For the parametrizations RRTMG and NewGoddard, the sensitivity in simulation of RE_{dif} increases and decreases by rising and reducing the value of the surface albedo, respectively. The change associated with the change in the surface albedo, however, is quite small, but slightly more noticeable in NewGoddard simulations. The change in the surface albedo has a reverse and similar effect in the sensitivity of the parameterization FLG under the cases I-a and L-a, respectively. This adverse effect is due to the fact that for the range of OD studied, the change in the surface albedo has a very little effect on the ΔRE_{dif} compared to $\overline{RE}_{dif}$. At OD = 1, for instance the values of ΔRE_{dif} obtained from FLG simulations for surface albedos of 0.04 and 0.40 for the case I-a are equal to 136 and 142 W m^{-2}, respectively. At the same OD, the corresponding values of $\overline{RE}_{dif}$ are 262 and 299 W m^{-2}, respectively. However, in case of the parameterizations RRTMG and NewGoddard, the situation is reverse. In case of the total irradiance, Figure 5 shows that all parameterizations for both cases have higher and lower sensitivities to different treatments of the transition zone for larger and smaller values of the surface albedo, respectively.

From the data provided in Figure 5 it can also be seen that all of the parameterizations for both cases have a lower sensitivity in simulation of direct and total irradiances at a higher solar zenith angle. Accordingly, all of the parameterizations under both cases (except FLG under the case I-a) have a higher sensitivity to different treatments of the transition zone.

5. Conclusions

The main objective of the present study was to investigate the differences in the broadband shortwave RE (Radiative Effect on surface irradiance) simulated by a meteorological/weather forecasting model, if a situation corresponding to the cloud-aerosol transition zone is assumed as either cloud or aerosol. To this aim, the shortwave parameterizations NewGoddard, RRTMG, and FLG included in the model WRF-ARW were isolated and adapted for ideal one-dimensional vertical simulations. These parameterizations were then utilized to perform a number of simulations under ideal cloud and aerosol modes, for different values of (i) cloud optical depths resulting from different sizes of crystals/droplets and mixing ratios (to describe water or ice content); and (ii) different aerosol optical depths combined with various aerosol types. These tests were carried out for two cases: the transition zone between ice clouds and aerosols (I-a) and between Liquid clouds and aerosols (L-a). The results obtained in this study can be summarized as follows:

1. As expected, for all the parameterizations, increasing cloud/aerosol particle optical depth leads to increasing (negative) effect in direct radiation component and increasing (positive) effect in diffuse component. The effect on the direct component dominates over effect in diffuse, thus leading to a negative effect in total radiation. However, there are differences among the radiative effects simulated by the parameterizations, which can be more dominantly seen in diffuse irradiance, compared to other radiation components.
2. Although there are differences among the radiative effects simulated by the parameterizations, the sensitivity involved with different assumptions of a situation regarding to the transition zone is quite substantial for all of them and it increases with optical depth. Based on the simulations performed for different solar zenith angles and surface albedos, regardless of the parameterizations utilized, different assumptions about the transition zone will lead to a mean relative radiative effect sensitivity ($\overline{\mathrm{R\Delta RE}}$) of 10–57, 32–115, and 50–169% in simulation of direct, diffuse, and total irradiances (see Figure 5).
3. Among the parameterizations studied, FLG was the least sensitive parameterization to different treatments of the transition zone for simulating diffuse and total irradiances ($\overline{\mathrm{R\Delta RE}}_{\mathrm{dif}}$ = 32–52% and $\overline{\mathrm{R\Delta RE}}_{\mathrm{t}}$ = 50-141%). In simulation of diffuse irradiance, the highest sensitivity was observed in the parameterizations RRTMG ($\overline{\mathrm{R\Delta RE}}_{\mathrm{dif}}$ = 105–160%). On the other hand, NewGoddard shows the highest sensitivity in simulations of direct irradiance ($\overline{\mathrm{R\Delta RE}}_{\mathrm{dir}}$ = 34–57%). Despite parameterizations, NewGoddard and RRTMG show different sensitivities (i.e., induce different uncertainties) to simulation of direct and diffuse irradiances, they have an almost similar (and high) sensitivity in the resulting total irradiance ($\overline{\mathrm{R\Delta RE}}_{\mathrm{t}}$ ranges between 102–169% and 105–161% for parameterizations NewGoddard and RRTMG, respectively).
4. For all the parameterizations and under all tested model configurations (different solar zenith angles and surface albedos) direct and total irradiances were the least and most sensitive irradiances to different treatments of the transition zone, respectively.
5. The previously mentioned sensitivities, i.e. differences in the radiative effect of the transition zone depending on the assumed treatment, dominantly result from the difference between results for clouds and aerosols (different types), not from cloud type or droplet/crystal size.

These results show that different treatments of the transition zone may lead to substantial uncertainties in simulation of direct, total, and diffuse irradiances and underline the importance of investigating the radiative effects of the transition zone, as the radiation field is of essential importance in meteorological and climate models. This means assuming the state of sky as either cloudy or cloud-free (neglecting the transition zone) may introduce large uncertainties to estimation of swrad reaching the Earth surface and thus the surface energy balance. This simplified assumption about the state of sky also leads to a large difference in the atmospheric shortwave heating rate which will influence the dynamics of the meteorological model. Results also suggest that the magnitude of these uncertainties is higher when parameterizations which cope with the

Radiative Transfer Equation in more detail (RRTMG and NewGoddard) are employed. Indeed, although complex (detailed) parameterizations are expected to have better performance and more accurate estimations, they are very sensitive to input variables. So that, in a situation corresponding to the transition zone (where the characteristics of the particle suspension are not well defined), an inaccurate assumption about these characteristics may lead to large uncertainties in the simulations when RRTMG or NewGoddard are applied ($\overline{R\Delta RE}_t > 102\%$,). Whereas, the uncertainties obtained from different assumptions of the transition zone are smaller (but still substantial, $\overline{R\Delta RE}_t > 50\%$) when the simpler parameterization FLG is utilized. These findings encourage further investigation on the transition zone from different aspects: (i) developing automated methods for detection of a situation regarding to transition zone (based on surface/satellite measurements) to facilitate studying the its actual radiative effects, (ii) the role and effects of transition zone in the Earth climate system, (iii) exploring the radiative effects of the transition zone in the longwave range, (iv) influence of not considering the transition zone on model dynamics.

Acknowledgments
The source codes of WRF-ARW model version 4.0 used in this study are freely accessible (http://www2.mmm.ucar.edu/wrf/users/download/get_source.html). The authors would like to kindly thank the Generalitat de Catalunya (Secretaria d'Universitats i Recerca) and European Union for providing the FI-AGAUR PhD grant (2018FI_B_00830). The authors would also like to thank the editor and the anonymous reviewers for their comments, which have been helpful to improve the paper.

References

Anderson, G. P., Clough, S. A., Kneizys, F. X., Chetwynd, J. H., & Shettle, E. P. (1986). *AFGL atmospheric constituent profiles (0.120 km)*. AIR FORCE GEOPHYSICS LAB HANSCOM AFB MA.

Baek, S. (2017). A revised radiation package of G-packed McICA and two-stream approximation: Performance evaluation in a global weather forecasting model. *Journal of Advances in Modeling Earth Systems*, *9*, 1628–1640. https://doi.org/10.1002/2017MS000994

Blossey, P. N., Bretherton, C. S., Zhang, M., Cheng, A., Endo, S., Heus, T., et al. (2013). Marine low cloud sensitivity to an idealized climate change: The CGILS les intercomparison. *Journal of Advances in Modeling Earth Systems*, *5*, 234–258. https://doi.org/10.1002/jame.20025

Bohren, C. F., & Huffman, D. R. (1998). Absorption and scattering of light by small particles. https://doi.org/10.1002/9783527618156

Calbó, J., Long, C. N., González, J. A., Augustine, J., & McComiskey, A. (2017). The thin border between cloud and aerosol: Sensitivity of several ground based observation techniques. *Atmospheric Research*, *196*(May), 248–260. https://doi.org/10.1016/j.atmosres.2017.06.010

Carslaw, K. S., Lee, L. A., Reddington, C. L., Pringle, K. J., Rap, A., Forster, P. M., et al. (2013). Large contribution of natural aerosols to uncertainty in indirect forcing. *Nature*, *503*(7474), 67–71. https://doi.org/10.1038/nature12674

Chen, M., Rood, R. B., & Takacs, L. L. (1997). Impact of a semi-Lagrangian and an Eulerian dynamical core on climate simulations. *Journal of Climate*, *10*(9), 2374–2389. https://doi.org/10.1175/1520-0442(1997)010<2374:IOASLA>2.0.CO;2

Chou, M.-D., & Suarez, M. J. (1999). A solar radiation parameterization (CLIRAD-SW) for atmospheric studies. *NASA Technical Memorandum*, *15*, 44. Retrieved from. http://www2.mmm.ucar.edu/wrf/users/phys_refs/SW_LW/Goddard_part1.pdf

Collins, W. D., Bitz, C. M., & Blackmon, M. L. (2006). The Community Climate System Model version 3 (CCSM3). *Journal of Climate*, *3*, 2122–2143. https://doi.org/10.1175/JCLI3761.1

Doubrawa, P., Montornès, A., Barthelmie, R. J., Pryor, S. C., & Casso, P. (2018). Analysis of different gray zone treatments in WRF-LES real case simulations. *Wind Energ. Sci. Discuss*, (January), 1–23. https://doi.org/10.5194/wes-2017-61

Dudhia, J. (1989). Numerical study of convection observed during the Winter Monsoon Experiment using a mesoscale two-dimensional model. *Journal of the Atmospheric Sciences*, *46*(20), 3077–3107. https://doi.org/10.1175/1520-0469(1989)046<3077:NSOCOD>2.0.CO;2

Fan, J., Wang, Y., Rosenfeld, D., & Liu, X. (2016). Review of aerosol–cloud interactions: Mechanisms, significance, and challenges. *Journal of the Atmospheric Sciences*, *73*(11), 4221–4252. https://doi.org/10.1175/JAS-D-16-0037.1

Fels, S. B., & Schwarzkopf, M. D. (1981). An efficient, accurate algorithm for calculating CO $_2$ 15 μm band cooling rates. *Journal of Geophysical Research*, *86*(C2), 1205. https://doi.org/10.1029/JC086iC02p01205

Fu, Q. (1996). An accurate parameterization of the solar radiative properties of cirrus clouds for climate models. *Journal of Climate*, *9*, 2058–2082.

Fuchs, J., & Cermak, J. (2015). Where aerosols become clouds-potential for global analysis based on CALIPSO data. *Remote Sensing*, *7*(4), 4178–4190. https://doi.org/10.3390/rs70404178

González, J. A., Calbó, J., & Sanchez-Romero, A. (2017). Measuring fast optical depth variations in cloud edges with a CCD-array spectrometer. *AIP Conference Proceedings*, *1810*. https://doi.org/10.1063/1.4975534

Gu, Y., Liou, K. N., Ou, S. C., & Fovell, R. (2011). Cirrus cloud simulations using WRF with improved radiation parameterization and increased vertical resolution. *Journal of Geophysical Research*, *116*, D06119. https://doi.org/10.1029/2010JD014574

Hu, Y. X., & Stamnes, K. (1993). An accurate parameterization of the radiative properties of water clouds suitable for use in climate models. *Journal of Climate*, *6*(4), 728–742. https://doi.org/10.1175/1520-0442(1993)006<0728:AAPOTR>2.0.CO;2

Huang, Y., & Wang, Y. (2019). How does radiation code accuracy matter? *Journal of Geophysical Research: Atmospheres*, *124*(20), 10,742–10,752. https://doi.org/10.1029/2019jd030296

Iacono, M. J., Delamere, J. S., Mlawer, E. J., Shephard, M. W., Clough, S. A., & Collins, W. D. (2008). Radiative forcing by long-lived greenhouse gases: Calculations with the AER radiative transfer models. *Journal of Geophysical Research*, *113*, D13103. https://doi.org/10.1029/2008JD009944

Jimenez, P. A., Hacker, J. P., Dudhia, J., Haupt, S. E., Ruiz-Arias, J. A., Gueymard, C. A., et al. (2016). WRF-SOLAR: Description and clear-sky assessment of an augmented NWP model for solar power prediction. *Bulletin of the American Meteorological Society*, *97*(7), 1249–1264. https://doi.org/10.1175/BAMS-D-14-00279.1

Joseph, J. H., Wiscombe, W. J., & Weinman, J. A. (1976). The delta-Eddington approximation for radiative flux transfer. *Journal of the Atmospheric Sciences*, *33*(12), 2452–2459. https://doi.org/10.1175/1520-0469(1976)033<2452:tdeafr>2.0.co;2

Koren, I., Feingold, G., Jiang, H., & Altaratz, O. (2009). Aerosol effects on the inter-cloud region of a small cumulus cloud field. *Geophysical Research Letters*, *36*, L14805. https://doi.org/10.1029/2009GL037424

Koren, I., Remer, L. A., Kaufman, Y. J., Rudich, Y., & Martins, J. V. (2007). On the twilight zone between clouds and aerosols. *Geophysical Research Letters*, *34*, L08805. https://doi.org/10.1029/2007GL029253

Lin, W., Liu, Y., Vogelmann, A. M., Fridlind, A., Endo, S., Song, H., et al. (2015). RACORO continental boundary layer cloud investigations: 3. separation of parameterization biases single-column model CAM5 simulations of shallow cumulus. *Journal of Geophysical Research: Atmospheres*, *120*, 6015–6033. https://doi.org/10.1002/2014JD022524

Liou, K.-N., Fu, Q., & Ackerman, T. P. (1988). A simple formulation of the delta-four-stream approximation for radiative transfer parameterizations. *Journal of Atmospheric Science*, *45*(13), 1940–1948. https://doi.org/10.1175/1520-0469(1988)045<1940:ASFOTD>2.0.CO;2

Loeb, N. G., Yang, P., Rose, F. G., Hong, G., Sun-Mack, S., Minnis, P., et al. (2018). Impact of ice cloud microphysics on satellite cloud retrievals and broadband flux radiative transfer model calculations. *Journal of Climate*, *31*(5), 1851–1864. https://doi.org/10.1175/JCLI-D-17-0426.1

Menang, K. P. (2018). Assessment of the impact of solar spectral irradiance on near-infrared clear-sky atmospheric absorption and heating rates. *Journal of Geophysical Research: Atmospheres*, *123*, 6460–6468. https://doi.org/10.1029/2018JD028342

Ming, Y., & Held, I. M. (2018). Modeling water vapor and clouds as passive tracers in an idealized GCM. *Journal of Climate*, *31*(2), 775–786. https://doi.org/10.1175/JCLI-D-16-0812.1

Moeng, C.-H., Dudhia, J., Klemp, J., & Sullivan, P. (2007). Examining two-way grid nesting for large eddy simulation of the PBL Using the WRF Model. *Monthly Weather Review*, *135*(6), 2295–2311. https://doi.org/10.1175/MWR3406.1

Montornès, A., Codina, B., & Zack, J. W. (2015). Analysis of the ozone profile specifications in the WRF-ARW model and their impact on the simulation of direct solar radiation. *Atmospheric Chemistry and Physics*, *15*(5), 2693–2707. https://doi.org/10.5194/acp-15-2693-2015

Montornès, A., Codina, B., Zack, J. W., & Sola, Y. (2016). Implementation of Bessel's method for solar eclipses prediction in the WRF-ARW model. *Atmospheric Chemistry and Physics*, *16*(9), 5949–5967. https://doi.org/10.5194/acp-16-5949-2016

Petty, G. W. (1958). *A first course on atmospheric radiation. Sundog Publishing*, (2nd ed.). Madison, Wisconsin: Sundog Publishing. https://doi.org/10.1029/2004eo360007

Powers, J. G., Klemp, J. B., Skamarock, W. C., Davis, C. A., Dudhia, J., Gill, D. O., et al. (2017). The weather research and forecasting model: Overview, system efforts, and future directions. *Bulletin of the American Meteorological Society*, *98*(8), 1717–1737. https://doi.org/10.1175/BAMS-D-15-00308.1

Ruiz-Arias, J. A., Dudhia, J., Santos-Alamillos, F. J., & Pozo-Vázquez, D. (2013). Surface clear-sky shortwave radiative closure intercomparisons in the Weather Research and Forecasting model. *Journal of Geophysical Research: Atmospheres*, *118*, 9901–9913. https://doi.org/10.1002/jgrd.50778

Schwarz, K., Cermak, J., Fuchs, J., & Andersen, H. (2017). Mapping the twilight zone – What we are missing between clouds and aerosols. *Remote Sensing*, *9*(6), 1–10. https://doi.org/10.3390/rs9060577

Seinfeld, J. H., Bretherton, C., Carslaw, K. S., Coe, H., DeMott, P. J., Dunlea, E. J., et al. (2016). Improving our fundamental understanding of the role of aerosol−cloud interactions in the climate system. *Proceedings of the National Academy of Sciences*, *113*(21), 5781–5790. https://doi.org/10.1073/pnas.1514043113

Skamarock, W. C., Klemp, J. B., Dudhia, J., Gill, D. O., Barker, D. M., Duda, M. G., ... Powers, J. G. (2008). A description of the advanced research WRF Version 3. *Technical Report*, (June), 113. https://doi.org/10.5065/D68S4MVH

Slingo, A. (1989). A GCM parameterization for shortwave radiative properties of water clouds. *Journal of the Atmospheric Sciences*, *46*(10), 1419–1427. https://doi.org/10.1175/1520-0469(1989)046<1419:AGPFTS>2.0.CO;2

Slingo, A., & Schrecker, H. M. (1982). On the shortwave radiative properties of stratiform water clouds. *Quarterly Journal of the Royal Meteorological Society*, *108*(456), 407–426. https://doi.org/10.1002/qj.49710845607

Tao, W. K., Anderson, D., Chern, J., Entin, J., Hou, A., Houser, P., et al. (2009). The Goddard multi-scale modeling system with unified physics. *Annales Geophysicae*, *27*(8), 3055–3064. https://doi.org/10.5194/angeo-27-3055-2009

Várnai, T., & Marshak, A. (2011). Global CALIPSO observations of aerosol changes near clouds. *IEEE Geoscience and Remote Sensing Letters*, *8*(1), 19–23. https://doi.org/10.1109/LGRS.2010.2049982

Várnai, T., & Marshak, A. (2015). Effect of cloud fraction on near-cloud aerosol behavior in the MODIS atmospheric correction ocean color product. *Remote Sensing*, *7*(5), 5283–5299. https://doi.org/10.3390/rs70505283

Wang, H., Skamarock, W. C., & Feingold, G. (2009). Evaluation of scalar advection schemes in the Advanced Research WRF Model using large-eddy simulations of aerosol–cloud interactions. *Monthly Weather Review*, *137*(8), 2547–2558. https://doi.org/10.1175/2009MWR2820.1

Yamaguchi, T., & Feingold, G. (2012). Technical note: Large-eddy simulation of cloudy boundary layer with the Advanced Research WRF model. *Journal of Advances in Modeling Earth Systems*, *4*, M09003. https://doi.org/10.1029/2012MS000164

Zdunkowski, W. G., Welch, R. M., & Korb, G. (1980). An investigation of the structure of typical two-stream-methods for the calculation of solar fluxes and heating rates in clouds. *Beiträge Zur Physik Der Atmosphäre*, *53*(2), 147–166.

Zhong, X., Ruiz-Arias, J. A., & Kleissl, J. (2016). Dissecting surface clear sky irradiance bias in numerical weather prediction: Application and corrections to the New Goddard Shortwave Scheme. *Solar Energy*, *132*, 103–113. https://doi.org/10.1016/j.solener.2016.03.009

Erratum

Due to typesetting errors, the Δ was omitted from or incorrectly italicized in in-line math throughout the originally published version of this article, and equations (2), (3), and (5) featured typographical errors. These errors have been corrected, and this may be considered the official version of record.